The Effect of the Side Chain of Acrylate Comonomers on the Orientation, Pore-Size Distribution, and Properties of Polyacrylonitrile Precursor and Resulting Carbon Fiber

JIN-SHY TSAI* and CHUNG-HUA LIN

Graduate Institute of Textile Engineering, Feng Chia University, Taichung, Taiwan, Republic of China

SYNOPSIS

The side-chain size of acrylate comonomer in polyacrylonitrile (PAN) precursor markedly influences the microstructure of PAN fiber and its resulting carbon fiber. In this paper, we propose that the model of the crystal orientation of PAN precursor and its resulting carbon fiber can explain the effect of the side-chain size of acrylate comonomer on the orientation of PAN fiber and carbon fiber. When PAN precursor contains a larger side chain of comonomer, PAN precursor has the preferred crystal orientation and higher crystallinity and the orientation of its resulting carbon fiber unexpectedly decreases. This is because the larger the side chain is, the lower is the orientation of the amorphous region of PAN fiber; as a result, the average orientation after carbonization decreases. In the same mole fraction of comonomer, the carbon fiber based on PAN precursor with a smaller side chain of acrylate comonomer has better mechanical properties and higher yield.

INTRODUCTION

Generally, it is believed[1] that in order to produce high-modulus carbon fibers from any given precursor it is essential to have a high preferred orientation of the ribbons in a direction parallel to the fiber axis. The value of the young's modulus depends upon several factors. The two most important are[2-4]

(a) Degree of orientation.
(b) Degree of perfection of the crystallites.

Therefore, the better the orientation of the crystallites, the higher is the value of the ultimate young's modulus. As far as polyacrylonitrile precursor is concerned, the molecular orientation can be brought about by stretching the fiber at various stages of development, namely:

(a) Spinning of the polyacrylonitrile precursor.
(b) Low-temperature stabilization.
(c) Graphitization.

The modulus and the strength of the PAN fiber increases with the stretch ratio during spinning.[5-8] The increase in preferred orientation on stretching is accompanied by an increase in crystal size.[9] If the fibers are not restrained during the early stages of pyrolysis, then length shrinkage and loss of preferred orientation occur.[10] This indicates that the modulus of carbon fibers made from oxidized PAN fibers increases with the increase in the length of the fibers during oxidation. During the carbonization, there is a quite marked improvement in orientation with increasing heat treatment temperature.[11]

From the results of mechanical properties,[5] it was shown that the tensile strengths and the young's modulus of the carbon fibers increase with the amount of stretch, thus reflecting a similar trend that had been present originally in the PAN fibers. Therefore, PAN fibers must have high tenacities or be highly oriented to serve as satisfactory precursors for carbon fibers. The results of our previous research[12] indicate that as the content of 2-ethyl hexyl acrylate comonomer in PAN precursor increases the PAN precursor has the preferred orientation and the orientation of its resulting carbon fiber decreases correspondingly.

* To whom correspondence should be addressed.

Journal of Applied Polymer Science, Vol. 42, 3039–3044 (1991)
 CCC 0021-8995/91/113039-06$04.00

Table I The Composition and Molecular Weight of PAN Precursors

Sample	Feed Composition (96.5 : 3.5 mol %)	Elemental Analysis (C%, N%, H%)	$\bar{M}_w \times 10^5$	$\bar{M}_w/\bar{M}_n$
PMA	AN : MA	67.02, 25.14, 5.81	2.8	1.6
PEA	AN : EA	66.81, 24.72, 5.92	2.7	1.6
PBA	AN : BA	67.45, 24.33, 6.26	2.8	1.6
PEHA	AN : EHA	67.87, 23.63, 6.45	2.7	1.6

MA = methyl acrylate; EA = ethyl acrylate; BA = butyl acrylate; EHA = 2-ethyl hexyl acrylate.

In this paper we will discuss how the group size of side chain of acrylate comonomers in PAN precursor affect the orientation, pore-size distribution, and properties of PAN precursor and its resulting carbon fiber.

EXPERIMENTAL

The PAN copolymers used in this study were polymerized in the mixed solvent of acetone and dimethyl sulfoxide at 60°C with α, α'-azobis (isobutyronitrile) as initiator under an inert atmosphere of nitrogen. The resulting polymerization solution was directly spun through a 10% DMSO coagulation bath at 5°C to form PAN precursor fiber, then stretched in boiling water and dried. PAN precursor was stabilized at 250°C for 30 min, then stabilized again at 270°C for 1 h in air, under 0.15 g/d tension. The oxidized PAN fiber was carbonized to 1200°C under a high-purity nitrogen atmosphere.

The average molecular weight and polydispersity ($\bar{M}_w/\bar{M}_n$) were determined by Waters model 440 gel-permeation chromatograph (eluting solvent: DMF containing 0.5 LiBr wt %; column: μ-Bondagel E-Linear). The molecular weight and distribution of PAN precursors are shown in Table I.

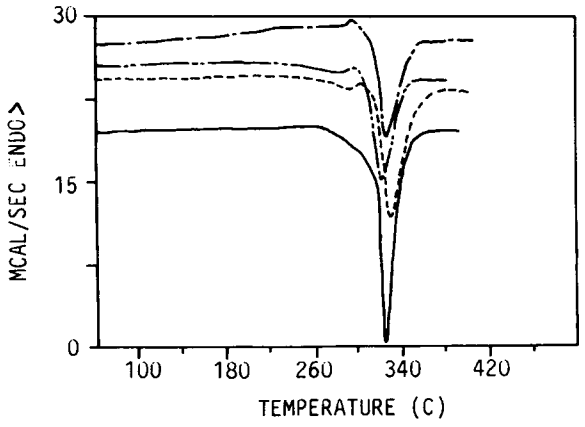

Figure 1 DSC curves of PAN precursors with different acrylate comonomer: (——) PMA; (- - -) PEA; (—·—) PBA; (—···—) PEHA.

The contents of carbon, nitrogen, and hydrogen in PAN precursor were determined by elemental analysis, which is shown in Table I, using a Carlo Erba elemental analyzer. The thermal properties of PAN precursors were obtained using a Perkin-Elmer system 7/4 differential scanning calorimeter. Samples were heated under air purge at a heating rate of 20°C/min.

X-ray data were determined by a Rigaku X-ray diffractometer using Ni-filtered CuK_α radiation. The crystallite size (Lc) was calculated from the following equation[13]:

$$Lc = \frac{K\lambda}{B \cos \theta}$$

where λ is the wavelength of CuK_α X-ray; B is the width at half-maximum intensity of the peak at $2\theta = 17°$ and 25° for PAN precursor and carbon fiber, respectively; and K is 0.89 (a constant).

The orientation of crystal was measured from the azimuthal scanning at $2\theta = 17°$ and 25° for PAN fiber and carbon fiber, respectively. The width at half-maximum intensity ($H° = I_{1/2}$) was used as an index of orientation, which may be used to calculate

Table II DSC Characterization of PAN Precursors

Sample	Temperature of Exothermic Peak (°C)	Exothermic Heat Per Unit Weight (cal/g)
PMA	321	−187
PEA	329	−150
PBA	326	−133
PEMA	320	−114

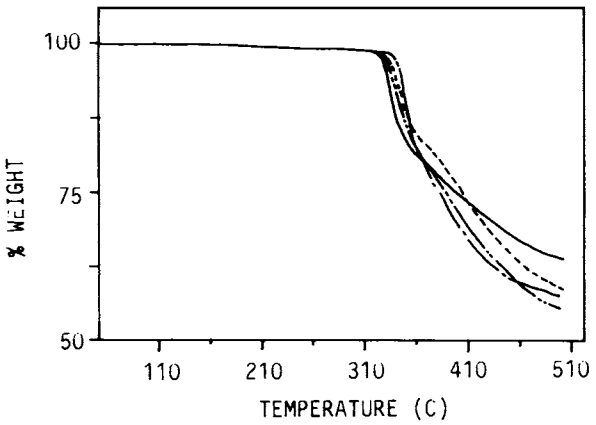

Figure 2 TGA curves of PAN precursors with different acrylate comonomer: (——) PMA; (- - -) PEA; (—·—) PBA; (—···—) PEHA.

the parallelism of the crystalline part of structure by the following equation[14,15]:

$$P = \frac{90 - H/2}{90} \times 100\%$$

The crystallinity index for PAN fiber was measured by Bell's method.[16] Mechanical properties of PAN fiber and carbon fiber were measured by a Microcomputer Universal Material Tester (Hung Ta Co., Ltd) Type 8104 at crosshead speed of 10 mm/min and 0.5 mm/min for PAN fiber and carbon fiber, respectively, with gauge length 20 mm and load cell of 30 g. Pore size of PAN fiber and carbon fiber were measured with a Micromeritics Autopore II 9220 using pressure from 0 to 55000 psia.

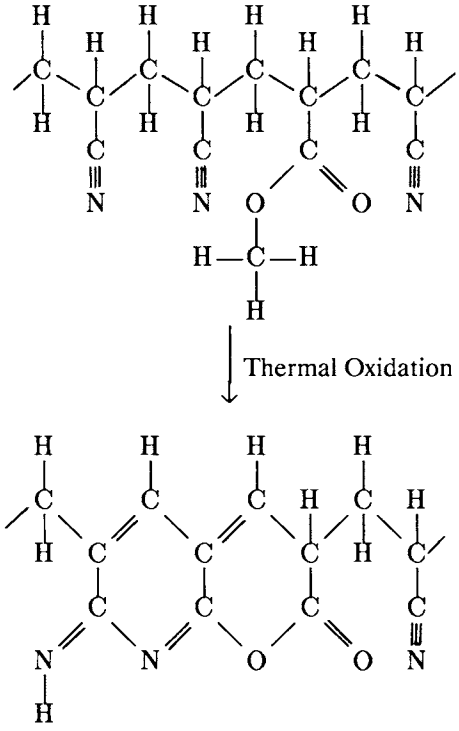

Figure 3 Concept of chemical structure containing cyclization and side-chain scission of comonomer in PAN precursor after oxidation.

RESULTS AND DISCUSSION

Thermal Properties

The DSC curves of various PAN precursors with different acrylate comonomer are shown in Figure 1. Sample PMA has the larger highness of peak due to the greater presence of CN group[17] (by weight), as is shown in Table I. Among them, the highness of the exothermic peak of sample PEHA is the lowest. This is attributed to the fact that PAN fiber contains a larger side chain of 2-ethyl hexyl acrylate; in the same mol fraction of comonomer, CN group content (by weight) decreases correspondingly. PAN fiber with the larger side chain of acrylate comonomer results in a decrease in exothermic heat as shown in Table II.

From the TGA curve, the yield of carbon fiber can be seen. PAN fiber with a larger side chain of

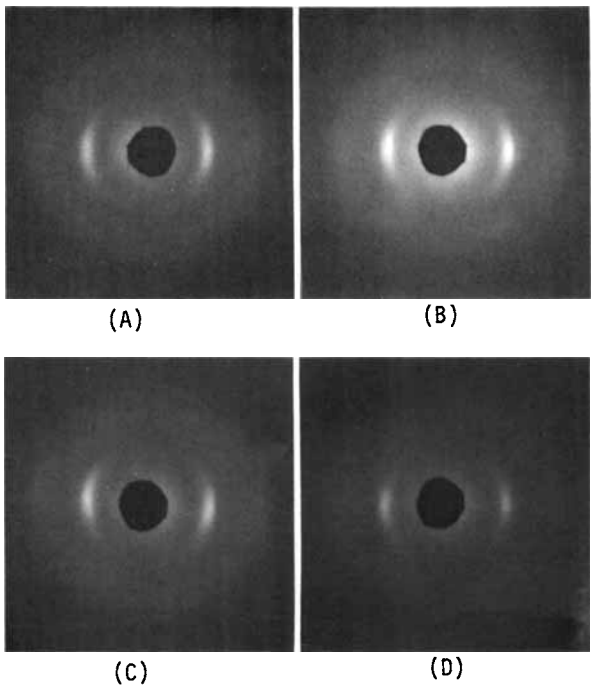

Figure 4 X-ray diffraction photographs of various PAN precursors: (A) PMA, (B) PEA, (C) PBA, (D) PEHA.

Table III Crystallinity and Orientation of PAN Precursors

Sample	Orientation (%)	Crystalline Size *Lc* (Å)	Crystallinity Index
PMA	78.7	29.4	0.69
PEA	80	29.5	0.70
PBA	83.5	30.2	0.72
PEHA	84.8	31.5	0.75

comonomer has a larger weight loss during carbonization (Fig. 2). This is because acrylate comonomer during cyclization at oxidized and carbonized stages results in the scission of side chain, as shown in Figure 3. Therefore, the larger the side chain of acrylate comonomer, the greater the weight loss of the resulting carbon fiber.

Crystal Orientation

Figure 4 shows X-ray diffraction photographs of various PAN precursors with different acrylate comonomer. In the photographs, the length of the arc indicates the orientation of crystal along the fiber axis. The width of the arc has a relationship with the grain size. Under the same spinning condition,

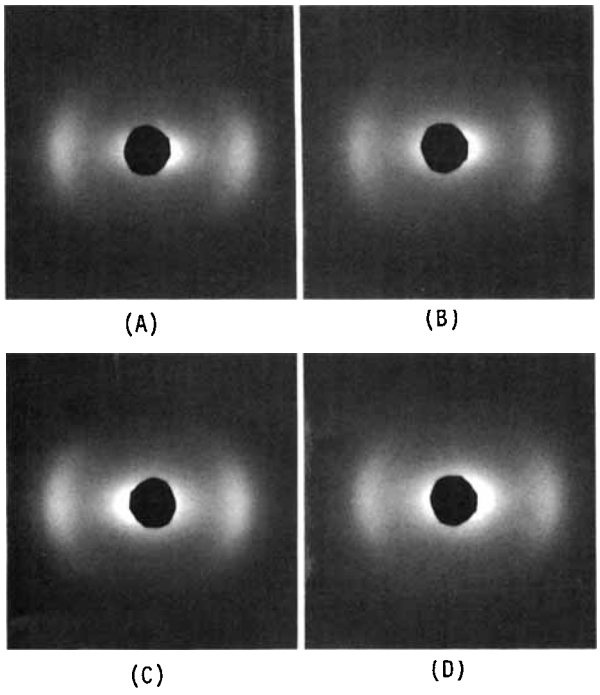

Figure 5 X-ray diffraction photographs of various carbon fibers: (A) PMA, (B) PEA, (C) PBA, (D) PEHA.

Table IV Crystalline Size and Orientation of Resulting Carbon Fiber

Sample	Orientation (%)	Crystalline Size (Å)
PMA	76	11.3
PEA	74.5	11.2
PBA	74.2	10.8
PEHA	73.2	10.3

the PAN precursor containing the larger side chain of acrylate comonomer has the preferred orientation, which causes the crystalline size and degree of crystallinity to become larger (Table III).

The X-ray diffraction photographs of their resulting carbon fibers are shown in Figure 5. It is interesting that the resulting carbon fiber made from PAN precursor with the preferred orientation has the imperfect orientation (Table IV).

From both orientation changes for PAN precursor and resulting carbon fiber, we propose a model, as shown in Figure 6, to explain the concept of orientation change during oxidation and carbonization. Molecular orientation in the amorphous region (B region in Fig. 6) for PAN precursor with the larger side chain of acrylate comonomer decreases, and the orientation in the crystal region (A part in Fig. 6) is preferred. Hence, the preferred orientation is obtained from a wide-angle X-ray only detecting the orientation of crystal and not detecting orientation in the amorphous. The amorphous region after oxidation brought about cyclization (part D in Fig. 6), which can be detected by X-ray due to the aromatic structure having intensity at $2\theta = 24$–$25°$. The average orientation involving parts C and D for resulting carbon fiber with the larger side chain of comonomer becomes lower, which is attributed the imperfect orientation in the D region.

Pore-size Distribution

In Table 5, it is apparent that an increase in the side-chain size of acrylate results in an increase in the median pore diameter among the polymer chains

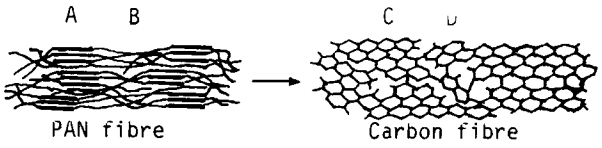

Figure 6 Orientation model for PAN precursor and carbon fiber.

Table V Pore Data of PAN Precursors

Sample	Total Intrusion Volume (mL/g)	Median Pore Diameter (μm)
PMA	3.25	0.0043
PEA	2.54	0.0042
PBA	1.91	0.0048
PEHA	1.89	0.0050

Table VI Pore Data of Resulting Carbon Fibers

Sample	Total Intrusion Volume (mL/g)	Median Pore Diameter (μm)
PMA	1.50	0.0037
PEA	1.48	0.0039
PBA	1.52	0.0040
PEHA	1.77	0.0040

of PAN precursor. This is because the amorphous region (B) with lower orientation has larger voids. In the same way, total intrusion volume (the amount of mercury intruded into voids) decreases, which is attributed to the crystal region (A) with preferred orientation having small voids or fewer small pores.

Figure 7 clearly shows that the large pores about 0.1 μm were spread in the amorphous region (B) containing a larger side chain of comonomer (2-ethyl hexyl acrylate) and that the small pores were mainly spread in the crystal region (A). Sample PMA has slightly smaller pores in the B region and slightly larger pores in the A region compared with sample PEHA.

The resulting carbon fiber carbonized from PAN precursor sample PEHA has a larger median pore diameter (Table VI), which is attributed to the larger pores in the D region of Figure 6, and total intrusion volume increases because of the chain scission of the larger side chain of comonomer. The pore-size distributions of various resulting carbon fibers are shown in Figure 8.

Mechanical Properties

The mechanical properties of fiber are affected mainly by the crystal characterization of fiber. Crystal changes from crystal (intensity at $2\theta = 17°$) for PAN fiber to crystal (at $2\theta = 24$–$25°$) for carbon fiber. PAN fiber (sample PEHA) with preferred orientation and higher crystallinity has higher modulus, lower elongation, and lower tensile strength, possibly due to the effect of larger pores, which is shown in Table VII. The modulus and tensile

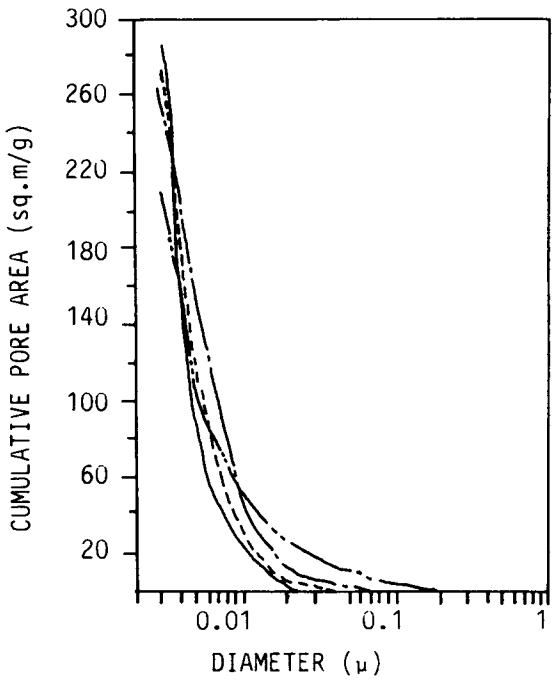

Figure 7 Pore-size distribution in PAN precursors: (——) PMA; (- - -) PEA; (—·—) PBA; (—··—) PEHA.

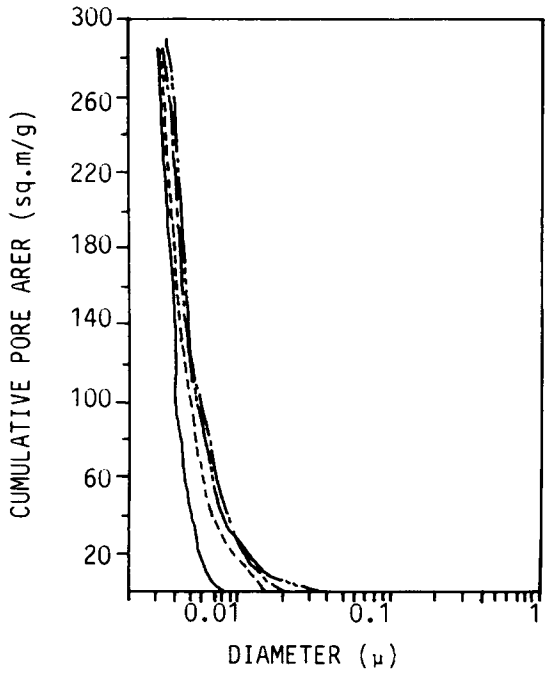

Figure 8 Pore-size distribution in carbon fibers: (——) PMA; (- - -) PEA; (—·—) PBA; (—··—) PEHA.

Table VII Mechanical Properties of PAN Precursors and Resulting Carbon Fibers

	PAN Fiber			Carbon Fiber		
Sample	Tensile Strength (g/d)	Modulus (g/d)	Elongation (%)	Tensile Strength (g/d)	Modulus (g/d)	Elongation (%)
PMA	4.58	88	16.40	13.70	1412	1.12
PEA	4.43	87	16.37	12.25	1268	1.02
PBA	4.48	114	15.70	11.91	1254	0.98
PEHA	3.98	115	12.94	11.15	1045	0.94

strength of resulting carbon fiber (sample PMA) increases with an increase in orientation and crystal size.

CONCLUSIONS

(a) The yield of resulting carbon fiber based on PAN precursor containing a larger side chain of acrylate comonomer decreased.

(b) The orientation of PAN precursor with a larger side chain of comonomer increases, and the orientation of its resulting carbon fiber decreases.

(c) In the same mole fraction of acrylate comonomer, the smaller the acrylate side chain of PAN precursor, the better the mechanical properties of its resulting carbon fiber.

We gratefully acknowledge the financial support of this research by Catalyst Research Center, China Technical Consultants, Inc. Our thanks are also due to Dr. Chin-Ling Liu, Mr. Su-Chi Hung, and Miss Der-Lin Ho (CRC/CTCI) for many valuable suggestions and support.

REFERENCES

1. R. J. Diefendorf and E. Tokarsky, *Polym. Eng. Sci.*, **15,** 150 (1975).
2. R. Bacon and W. A. Schalamon, *Appl. Polym. Symp.*, **9,** 285 (1969).
3. W. Watt, L. N. Phillips, and W. Johnson, *Engineer*, **May,** 27 (1966).
4. L. M. Manocha and O. P. Bahl, *Fibre Sci. Tech.*, **17,** 221 (1982).
5. R. Moreton, in *3rd. Conf. Industrial Carbon and Graphite,* 1970, p. 472.
6. James P. Bell and J. H. Dumbleton, *Text. Res. J.*, **February,** 196 (1970).
7. J. W. Johnson, J. R. Marjoram, and P. G. Rose, *Nature,* **221,** 357 (1969).
8. A. I. Stoyanov, *J. Appl. Polym. Sci.*, **24,** 583 (1979).
9. A. K. Gupta and R. P. Singhal, *J. Polym. Sci. Polym. Phys. Ed.*, **21,** 2243 (1983).
10. W. Watt and W. Johnson, *Appl. Polym. Symp.*, **9,** 215 (1969).
11. M. Lewin and J. Preston, *High Technology Fibers,* Marcel Dekker, New York and Basel, 1985, p. 185.
12. J.-S. Tsai and C.-H. Lin, *J. Appl. Polym. Sci.*, to appear.
13. B. D. Cullity, *Elements of X-ray Diffraction,* Addison-Wesley, Reading, MA, 1978, Chap. 3.
14. M. Takahashi, M. Watanabe, and Y. Kinoshita, *J. Soc. Text. Cellulose Ind. Jpn.*, **2,** 713 (1959).
15. M. Kakudo and N. Kasai, *X-Ray Diffraction by Polymers,* Kodansha, Elsevier, Tokyo, 1972, p. 254.
16. J. P. Bell and J. H. Dumbleton, *Text. Res. J.*, **41,** 196 (1971).
17. U. S. Pat. 3,814,577 (1974).

Received November 13, 1989
Accepted November 12, 1990